

IONIZATION EQUILIBRIUM TIMESCALES IN COLLISIONAL PLASMAS

RANDALL K. SMITH

Harvard-Smithsonian Center for Astrophysics
60 Garden St., Cambridge, MA 02138; rsmith@cfa.harvard.edu

JOHN P. HUGHES

Department of Physics and Astronomy, Rutgers University, Piscataway, NJ 08854-8019; jph@physics.rutgers.edu
Draft version June 3, 2010

ABSTRACT

Astrophysical shocks or bursts from a photoionizing source can disturb the typical collisional plasma found in galactic interstellar media or the intergalactic medium. The spectrum emitted by this plasma contains diagnostics that have been used to determine the time since the disturbing event, although this determination becomes uncertain as the elements in the plasma return to ionization equilibrium. A general solution for the equilibrium timescale for each element arises from the elegant eigenvector method of solution to the problem of a non-equilibrium plasma described by Masai (1984) and Hughes & Helfand (1985). In general the ionization evolution of an element Z in a constant electron temperature plasma is given by a coupled set of $Z+1$ first order differential equations. However, they can be recast as Z uncoupled first order differential equations using an eigenvector basis for the system. The solution is then Z separate exponential functions, with the time constants given by the eigenvalues of the rate matrix. The smallest of these eigenvalues gives the scale of slowest return to equilibrium independent of the initial conditions, while conversely the largest eigenvalue is the scale of the fastest change in the ion population. These results hold for an ionizing plasma, a recombining plasma, or even a plasma with random initial conditions, and will allow users of these diagnostics to determine directly if their best-fit result significantly limits the timescale since a disturbance or is so close to equilibrium as to include an arbitrarily-long time.

Subject headings: atomic data, atomic processes, plasmas

1. INTRODUCTION

Astrophysical plasma densities can have densities in the range of a few particles per cubic meter, resulting in interaction timescales of millions of years that create long delays between a thermodynamic event and its apparent consequences. For example, the ion populations in remnants created by the passage of supernova shocks are often well out of equilibrium with the electron temperature in the plasma (Itoh 1978; Gronenschild & Mewe 1982; Hamilton, Sarazin & Chevalier 1983). The general problem of calculating the evolution of such a plasma as a function of time, including the emission spectrum from the plasma during the evolution, requires a large collection of atomic data and a moderately complex spectral code. A number of such codes exist, such as the Raymond & Smith (1977) code, the Kaastra, Mewe & Nieuwenhuijzen (1996) (SPEX) code, and the Smith et al. (2001) (APEC) code.

Comparing observed X-ray spectra with these spectral models have been used to determine the 'age' of supernova remnants (SNR) (*e.g.* Harrus et al. 1997; Yatsu et al. 2005) or in the case of Cas A, to determine the when individual knots in the ejecta were shocked and thus follow the propagation of the original explosion (Hwang & Laming 2003). Although these examples are for ionizing plasmas, recent Suzaku observations have also shown that recombining plasmas can be found in SNR as well (Yamaguchi et al. 2009; Ozawa et al. 2009). Fitting the spectra of these non-equilibrium plasma returns the temperature and overall

density-weighted timescale of the plasma $n_e \times t$ (because all ionization and recombination rates scale with electron density n_e), but these fits contain no direct indication of how close this is to an equilibrium value for each element. As a result, the spectroscopist may estimate a result that is in fact best treated as a lower limit. The differences in elemental timescales amount to 'clocks' that operate over various ranges as each element returns to equilibrium, so with high-resolution spectra the sensitivity of the timescale measurement can be enhanced by focussing on specific elemental lines.

While modifying the APEC code to use a faster and more general ionization state calculation routine (described in §2), we noted that one useful side effect of this method was a direct measure of the timescale for obtaining both the first changes to the ion population and the final equilibrium ionization state for each atom regardless of initial conditions and assuming only that the plasma is held at constant electron temperature. These results are shown graphically in §3, and some consequences are given in §4.

2. METHOD

Masai (1984) and Hughes & Helfand (1985) described a fast method to calculate the ionization population of an atom using the eigenvectors and eigenvalues of the rate matrix equation. Restating for convenience the formalism set up in Hughes & Helfand (1985), the basic

equation is:

$$\frac{dF_i}{dt} = n_e(\alpha_{i-1}(T_e)F_{i-1} - [\alpha_i(T_e) + R_{i-1}(T_e)]F_i + R_i(T_e)F_{i+1}) \quad (1)$$

where F_i is the ion fraction of the i th ion with $i = 1$ the neutral case and $i = Z + 1$ the fully-stripped ion with atomic number Z . All the rates are proportional to the electron density n_e , which has been factored out. If n_e is not constant, this approach is still applicable using $n_e t$ as the independent variable. The ionization rate $\alpha_i(T_e)$, a function of the electron temperature T_e , gives the rate from state i to state $i + 1$, while the recombination rate $R_i(T_e)$ gives the rate from state $i + 1$ to i . This equation can then be rewritten in matrix form as

$$\frac{d\vec{F}}{dt} = -n_e \mathbf{A}(\mathbf{T}_e) \cdot \vec{F} \quad (2)$$

where \vec{F} is a vector with dimension $Z + 1$ of ion populations and $\mathbf{A}(\mathbf{T}_e)$ is the matrix of ionization and recombination rates. This matrix will have one zero eigenvalue, representing the equilibrium solution. This singularity may cause numerical problems that can be addressed using the normalization requirement that $\sum F_i = 1$ to reduce the matrix to $Z \times Z$ dimensions (see the Appendix of Hughes & Helfand (1985) for details). Since the method assumes the electron temperature is held constant, it is convenient to define $\vec{G} \equiv \vec{F} - \vec{F}^{eq}$, where \vec{F}^{eq} is the ion population in equilibrium at temperature T . Then we can rewrite Eq 2 as

$$\frac{d\vec{G}}{dt} = -n_e \mathbf{A}(\mathbf{T}_e) \cdot \vec{G}, \quad (3)$$

dropping the constant term $\mathbf{A}(\mathbf{T}_e) \cdot \vec{F}^{eq}$ as $d\vec{F}/dt = 0$ in equilibrium. This formulation has the advantage that $\lim_{t \rightarrow \infty} \vec{G} = 0$ by definition.

Then we can define $\mathbf{V}(\mathbf{T}_e)$ as the matrix of eigenvectors of $\mathbf{A}(\mathbf{T}_e)$ with eigenvalues $\vec{\lambda}$. Then setting $\vec{G}' \equiv \mathbf{V}(\mathbf{T}_e)^{-1} \vec{G}$ and $\mathbf{\Lambda} \equiv \vec{\lambda} \mathbf{I}$, we can write

$$\frac{d\vec{G}'}{dt} = -n_e \mathbf{\Lambda} \vec{G}' \quad (4)$$

with the solution $\vec{G}'(t) = \vec{c} \exp(-n_e \vec{\lambda} t)$ where \vec{c} is determined from the initial conditions. The values of \vec{G}' do not, of course, correspond to individual ions, although these can be easily recovered using $\vec{G} = \mathbf{V} \vec{G}'$. Expanding this for ion i , we see that

$$G_i(t) = \sum_j V_{ji} G'_j = \sum_j V_{ji} c_j \exp(-n_e \lambda_j t). \quad (5)$$

The requirement that $\lim_{t \rightarrow \infty} \vec{G} = 0$ implies that $\lambda_j > 0$ for all j . More importantly, however, Eq. 5 shows that the overall rate of approach to equilibrium will generally be dominated by the smallest eigenvalue λ_j , independent of the initial conditions. Conversely, the largest eigenvalue sets the minimum timescale for any significant change in the ion population.

3. RESULTS

Combining the result from §2 with existing ionization and recombination rates, we can calculate the actual timescales (e-folding times) for an astrophysical plasma to reach equilibrium. Figure 1 plots $\max\{1/\vec{\lambda}\}$, in units of $\text{cm}^{-3} \text{s}$ as a function of electron temperature for a range of astrophysically abundant elements. The companion Figure 2 shows $\min\{1/\vec{\lambda}\}$, effectively the timescale for any significant change in the ion population. These figures use the ionization and recombination rate from Mazzotta et al. (1998). These rates have been updated recently (Bryans et al. 2009); while important for spectral studies, the new rates are generally within 50% of the older values, not enough to significantly change these results. Figure 1 does show that the typical expectation that a plasma will reach equilibrium when $n_e t \sim \text{few} \times 10^{13} \text{ cm}^{-3} \text{s}$ is overly conservative. For most atoms, equilibrium will be achieved an order of magnitude earlier, or in the case of light ions such as C or O at high temperatures, two orders of magnitude or more.

4. DISCUSSION AND CONCLUSIONS

The complex structure that can be seen in Figure 1 is the result of different ions and different ionization/recombination rates dominating the process at different temperatures. An examination of the individual ion populations as a function of time showed that the most populous ion is often the slowest to reach equilibrium. At lower temperatures ($T = 10^4 - 10^6 \text{ K}$), a range of L-shell ions, with a range of ionization and recombination rates, dominate the final equilibrium state, leading to complex variations in the eigenvalues. However, at higher temperatures, the curves simplify as the ion population is dominated by He-like, hydrogenic, or bare ions. Figure 2 shows a simpler structure, albeit with one significant ‘kink’ for each atom. This feature arises as the ion population begins to contain a significant number of non-neutrals, and is correlated with the first ionization potential of each element.

Although Figure 1 cannot be used to calculate the ion population directly, it fills a long-standing need in the X-ray spectral community. It is particularly useful in that it is entirely independent of initial conditions, equally applicable to a neutral medium that is rapidly ionizing or tracking the recombination of a fully-stripped plasma. Figure 1 can easily be used to determine if the best-fit temperature and density-weighted time returned from the spectral fitting program implies a significantly non-equilibrium plasma or rather one near equilibrium, and to see which elements would be the most time-sensitive at a given temperature. Figure 2, in turn, shows that no ion population will be impacted by timescales less than $\sim 10^7 \text{ cm}^{-3} \text{s}$ and in some cases significantly longer. Although only collisional processes were included here, the method is general. A similar figure could be generated for a photoionized plasma held at constant photoionization parameter ξ , for example when studying a plasma near a quiescent X-ray binary after an outburst.

We thank the anonymous referee for suggesting determining the minimum timescale as well as the maximum,

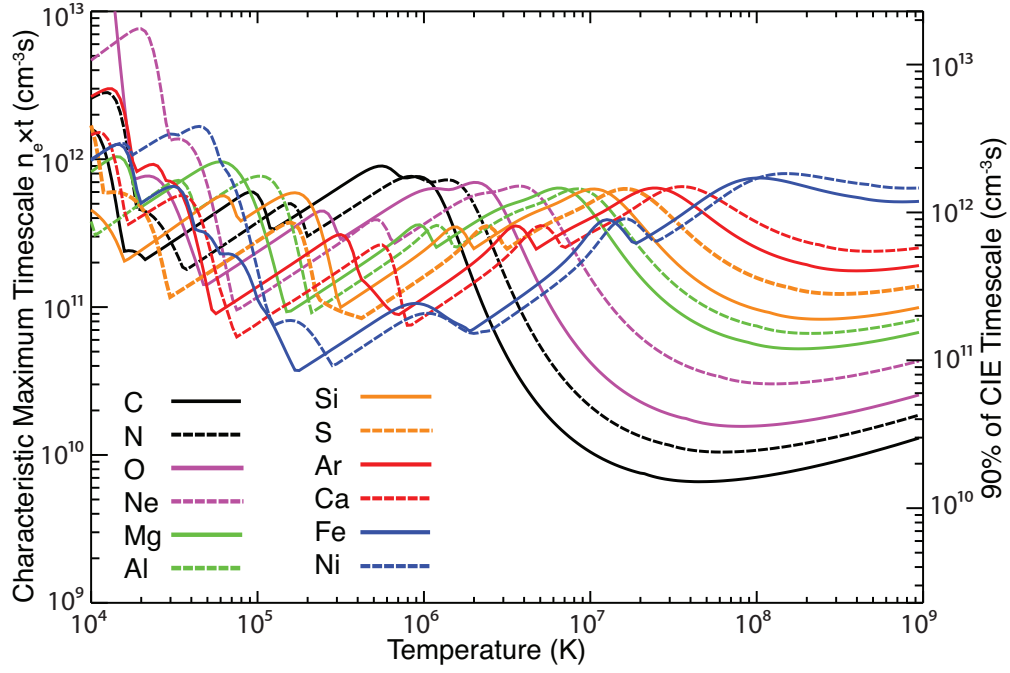


FIG. 1.— [Left axis] Density-weighted timescales (in units of $\text{cm}^{-3} \text{s}$) for C, N, O, Ne, Mg, Al, S, Si, Ar, Ca, Fe, and Ni to achieve one e-folding (e^{-1}) towards ionization equilibrium in a constant temperature plasma. [Right axis] Density-weighted timescale for all ions to be within 10% of their equilibrium value.

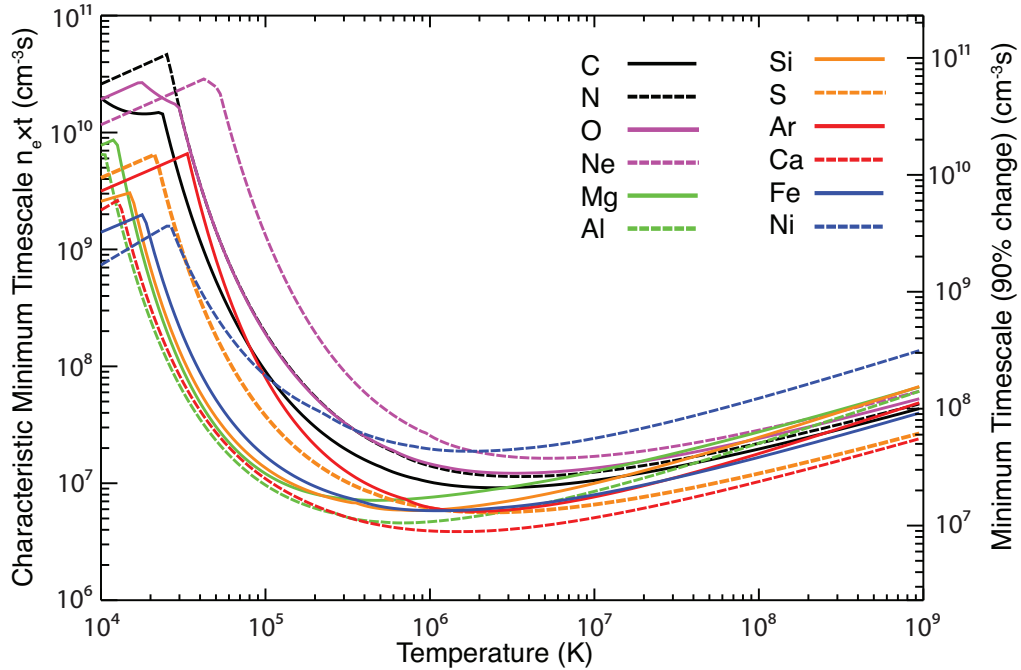


FIG. 2.— [Left axis] Density-weighted timescales (in units of $\text{cm}^{-3} \text{s}$) for C, N, O, Ne, Mg, Al, S, Si, Ar, Ca, Fe, and Ni to achieve one e-folding (e^{-1}) of any change in ionization state for an atom in a constant temperature plasma. [Right axis] Density-weighted timescale for an ionization state change of 90%.

and acknowledge helpful discussions with Terrance Gaetz

and John Raymond. Support for this project came from the Chandra GO Theory program, grant #TM4-5004X.

REFERENCES

- Bryans, P., Landi, E., & Savin, D. W. 2009, *ApJ*, 691, 1540
 Gronenschild, E. H. B. M. & Mewe, R. 1982, *A&AS*, 48, 305
 Hamilton, A. J. S., Sarazin, C. L. & Chevalier, R. 1983, *ApJS*, 51, 115
 Harrus, I. M., Hughes, J. P., Singh, K. P., Koyama, K., & Asaoka, I. 1997, *ApJ*, 488, 781
 Hughes, J. P. & Helfand, D. J. 1985, *ApJ*, 291, 544
 Hwang, U. & Laming, J. M. 2003, *ApJ*, 597, 362
 Itoh, H. 1978, *PASJ*, 30, 489
 Kaastra, J. S., Mewe, R., & Nieuwenhuijzen, H. 1996, "UV and X-ray Spectroscopy of Astrophysical and Laboratory Plasmas" eds. K. Yamashita and T. Watanabe. (Tokyo : Universal Academy Press), p.411
 Mazzotta, P., Mazzitelli, G., Colafrancesco, S., Vittorio, N. 1998, *A&AS*, 133, 403
 Masai, K. 1984, *Ap&SS*, 98, 367
 Ozawa, M., Koyama, K., Yamaguchi, H., Masai, K., & Tamagawa, T. 2009, *ApJ*, 706, L71
 Raymond, J. C. & Smith, B. 1977, *ApJ*, 35, 419
 Smith, R. K., Brickhouse, N. S., Liedahl, D. A., & Raymond, J. C. 2001, *ApJ*, 556, L91
 Yamaguchi, H., Ozawa, M., Koyama, K., Masai, K., Hiraga, J. S., Ozaki, M., & Yonetoku, D. 2009, *ApJ*, 705, L6
 Yatsu, Y., Kawai, N., Kataoka, J., Kotani, T., Tamura, K., & Brinkmann, W. 2005, *ApJ*, 631, 312